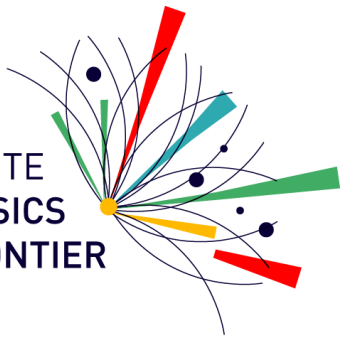


MILLENNIUM INSTITUTE
FOR SUBATOMIC PHYSICS
AT HIGH-ENERGY FRONTIER
SAPHIR



PONTIFICIA
UNIVERSIDAD
CATÓLICA
DE CHILE

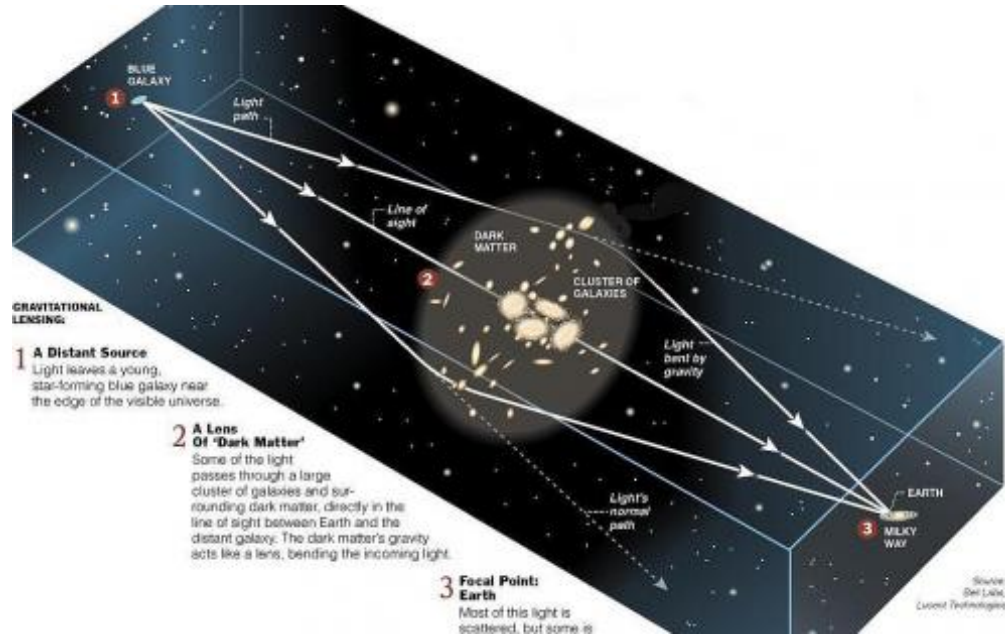
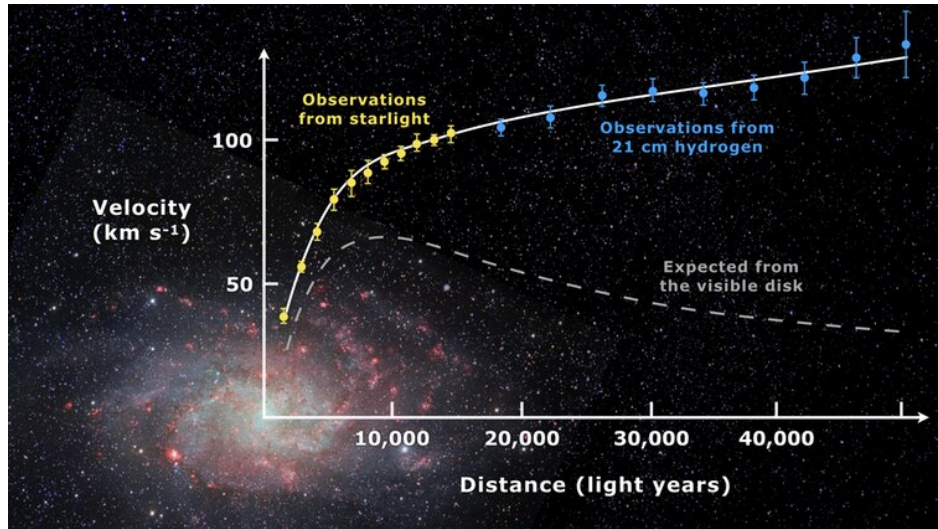
Particles and Space

Marco Aurelio Díaz

PUC



Dark Matter



Evidence for Dark Matter

- Rotation of galaxies
- Velocities of galaxies in clusters
- Velocities of stars in dwarf galaxies
- Hot gas in galaxy clusters
- Galaxy interactions
- Collisions of galaxy clusters
- Gravitational lensing

Cosmic Collision of 2 Galaxy Clusters splitting normal matter and dark matter apart

– Another Clear Evidence of Dark Matter –
(8/21/06)

The main image shows the collision of two galaxy clusters, with 'Ordinary Matter (NASA's Chandra X Observatory)' in yellow and 'Dark Matter (Gravitational Lensing)' in red. A yellow circle highlights a region where the dark matter is separated from the normal matter. A text box states: 'Approximately the same size as the Milky Way'. On the right, a vertical timeline labeled 'time' shows four stages (1-4) of the collision.

Neutrinos

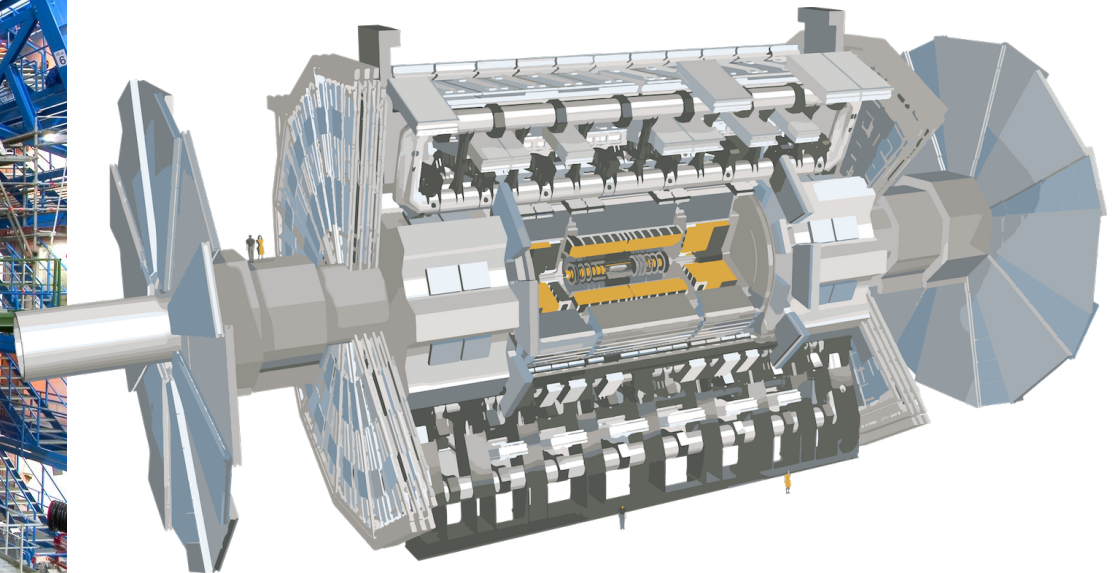
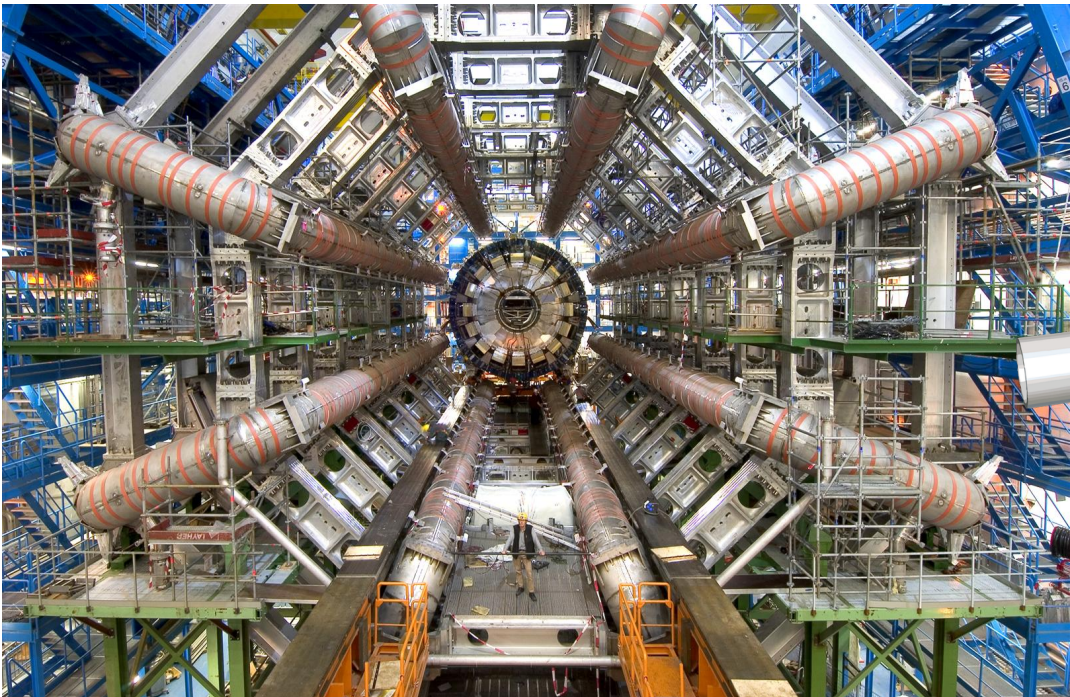
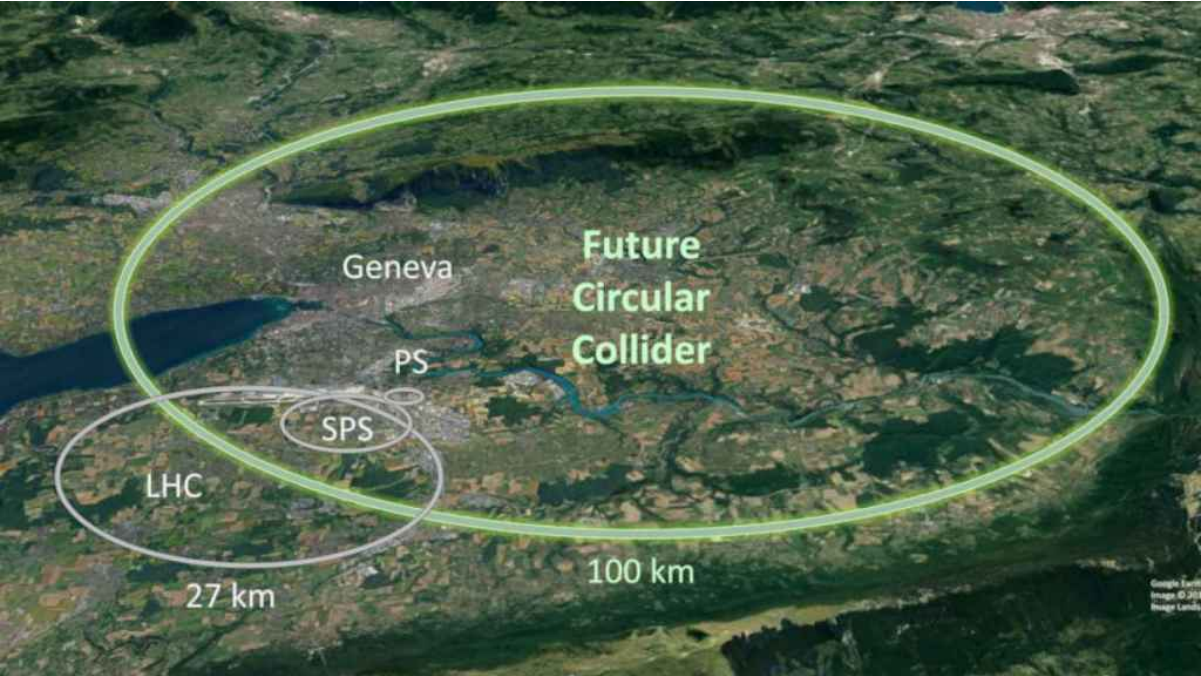
From:

JHEP **02**, 071 (2021),
 P.F. de Salas, D.V. Forero,
 S. Gariazzo,
 P. Martínez-Miravé,
 O. Mena, C.A. Ternes,
 M. Tórtola, J.W.F. Valle.

parameter	best fit $\pm 1\sigma$	2σ range	3σ range
$\Delta m_{21}^2 [10^{-5} \text{eV}^2]$	$7.50^{+0.22}_{-0.20}$	7.12–7.93	6.94–8.14
$ \Delta m_{31}^2 [10^{-3} \text{eV}^2]$ (NO)	$2.55^{+0.02}_{-0.03}$	2.49–2.60	2.47–2.63
$ \Delta m_{31}^2 [10^{-3} \text{eV}^2]$ (IO)	$2.45^{+0.02}_{-0.03}$	2.39–2.50	2.37–2.53
$\sin^2 \theta_{12} / 10^{-1}$	3.18 ± 0.16	2.86–3.52	2.71–3.69
$\theta_{12} / ^\circ$	34.3 ± 1.0	32.3–36.4	31.4–37.4
$\sin^2 \theta_{23} / 10^{-1}$ (NO)	5.74 ± 0.14	5.41–5.99	4.34–6.10
$\theta_{23} / ^\circ$ (NO)	49.26 ± 0.79	47.37–50.71	41.20–51.33
$\sin^2 \theta_{23} / 10^{-1}$ (IO)	$5.78^{+0.10}_{-0.17}$	5.41–5.98	4.33–6.08
$\theta_{23} / ^\circ$ (IO)	$49.46^{+0.60}_{-0.97}$	47.35–50.67	41.16–51.25
$\sin^2 \theta_{13} / 10^{-2}$ (NO)	$2.200^{+0.069}_{-0.062}$	2.069–2.337	2.000–2.405
$\theta_{13} / ^\circ$ (NO)	$8.53^{+0.13}_{-0.12}$	8.27–8.79	8.13–8.92
$\sin^2 \theta_{13} / 10^{-2}$ (IO)	$2.225^{+0.064}_{-0.070}$	2.086–2.356	2.018–2.424
$\theta_{13} / ^\circ$ (IO)	$8.58^{+0.12}_{-0.14}$	8.30–8.83	8.17–8.96
δ / π (NO)	$1.08^{+0.13}_{-0.12}$	0.84–1.42	0.71–1.99
$\delta / ^\circ$ (NO)	194^{+24}_{-22}	152–255	128–359
δ / π (IO)	$1.58^{+0.15}_{-0.16}$	1.26–1.85	1.11–1.96
$\delta / ^\circ$ (IO)	284^{+26}_{-28}	226–332	200–353

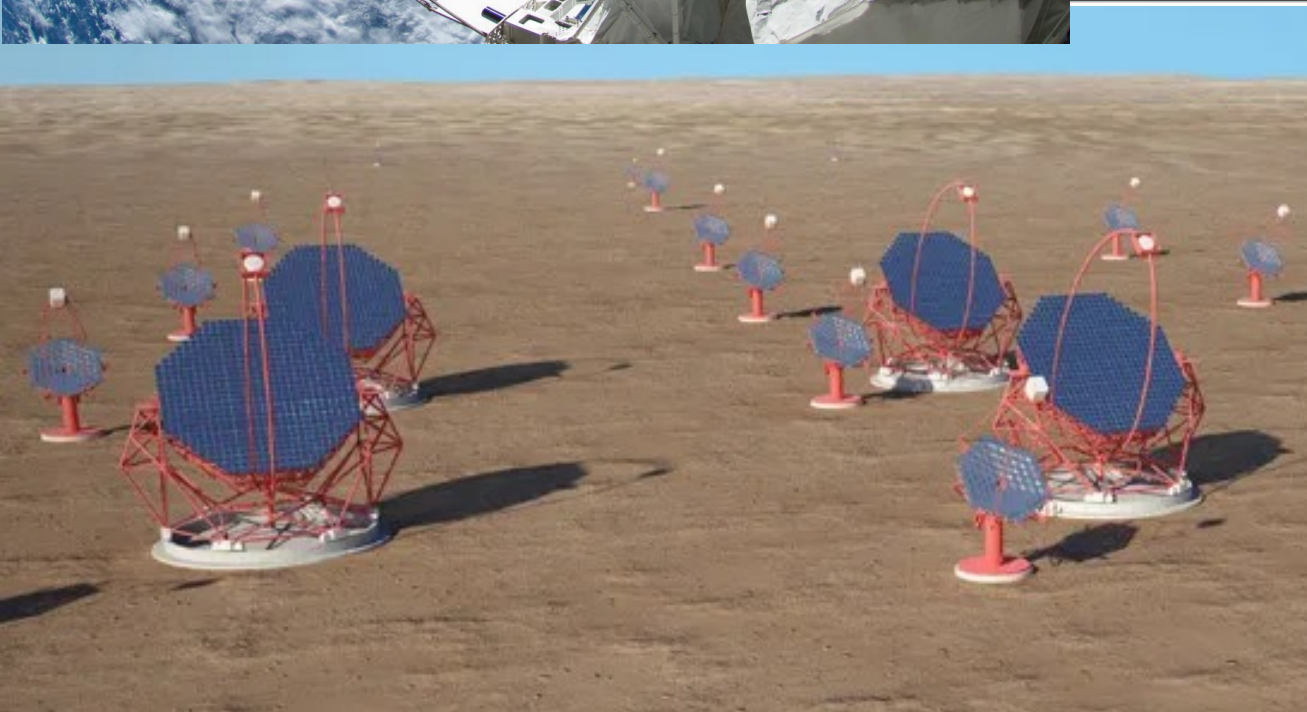


Colliders



Particles from Space

Our Sun (one of a billion stars in the Milky Way), and our solar system is located NOT in the center, and NOT at the edge, but about 2/3 out on a spiral arm.



Scotogenic Model

Due to E. Ma, *Phys. Rev D* **73**, 077301 (2006).

- 1.- Neutrino Masses (1 loop \Rightarrow small)
- 2.- Dark Matter (DM)

	Standard Model			Fermions	Scalar
	L	e	ϕ	N	η
$SU(2)_L$	2	1	2	1	2
Y	-1	-2	1	0	1
\mathbb{Z}_2	+	+	+	-	-
l	1	1	0	1	0

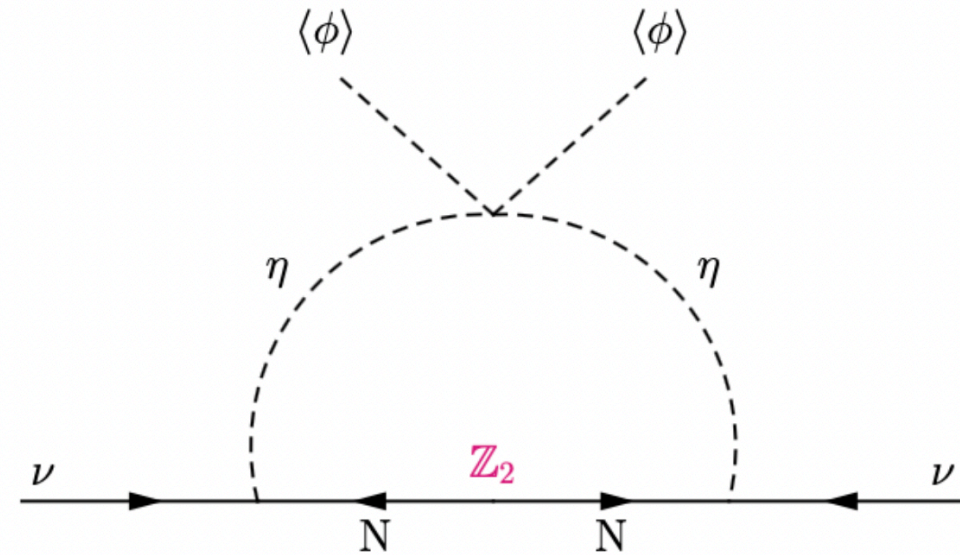
$$\mathcal{L} = -Y_N^{\alpha\beta} \bar{N}_\alpha \eta^\dagger L_\beta - \frac{1}{2} \bar{N}^\alpha M_{\alpha\beta} N^{\beta c} + \dots$$

$$m_\phi^2 = 2\lambda_1 v^2$$

$$m_{\eta^\pm}^2 = m_\eta^2 + \lambda_3 \frac{v^2}{2}$$

$$m_{\eta_R}^2 = m_\eta^2 + (\lambda_3 + \lambda_4 + \lambda_5) \frac{v^2}{2}$$

$$m_{\eta_I}^2 = m_\eta^2 + (\lambda_3 + \lambda_4 - \lambda_5) \frac{v^2}{2}$$

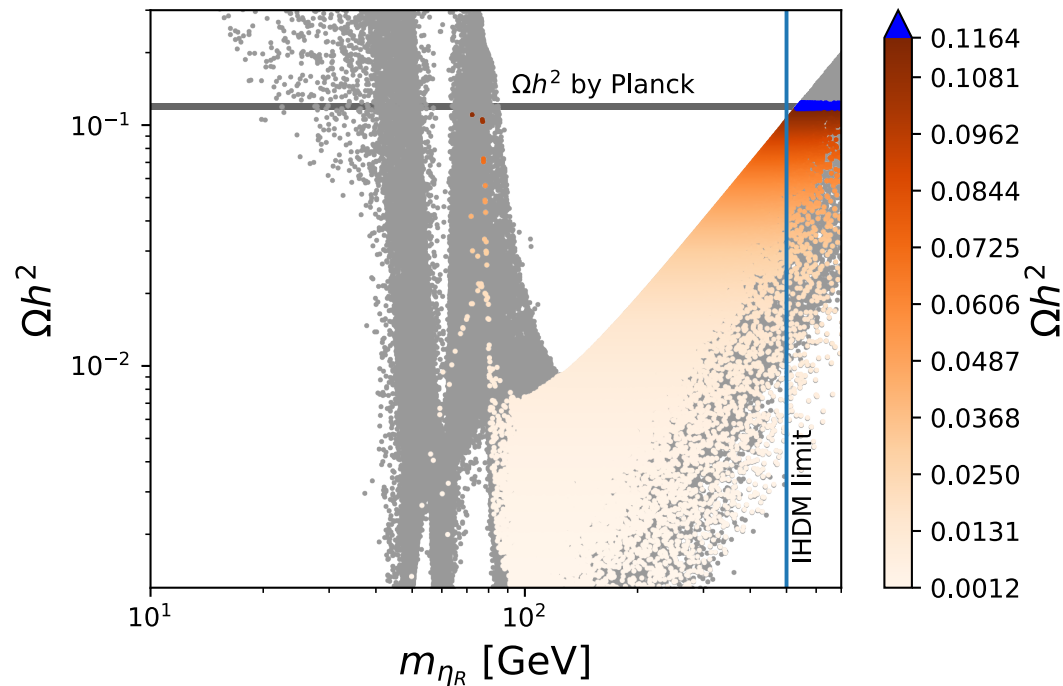
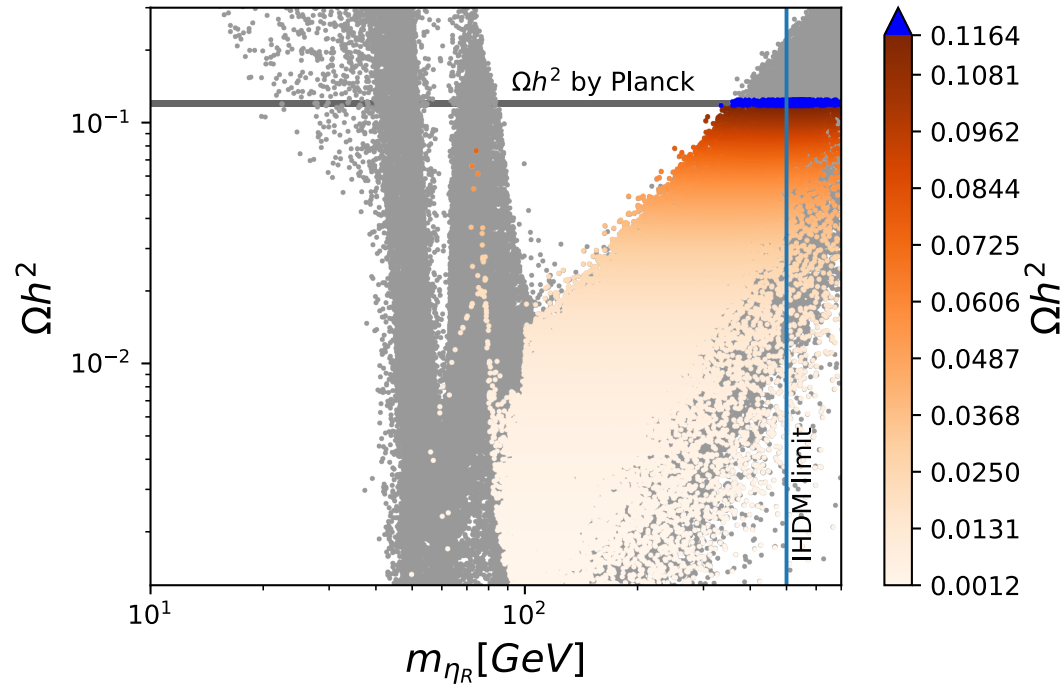


- DM: Real part of η (scalar DM)
- Look for long lived particles

$$V = m_\phi^2 \phi^\dagger \phi + m_\eta^2 \eta^\dagger \eta + \lambda_1 (\phi^\dagger \phi)^2 + \lambda_2 (\eta^\dagger \eta)^2 + \lambda_3 (\phi^\dagger \phi) (\eta^\dagger \eta) + \lambda_4 (\phi^\dagger \eta) (\eta^\dagger \phi) + \frac{\lambda_5}{2} ((\phi^\dagger \eta) + (\eta^\dagger \phi))^2$$

Based on *J. Phys. G* **49**, 6, 065001 (2022), in collaboration with Ivania Maturana-Avila and Giovanna Cottin.

Relic Density



Comparison of the relic density of DM in the Scotogenic model (top), with the Inert Higgs Doublet model (bottom).

The IHDM limit of about 500 GeV is reduced to about 300 GeV.

Parameter	Scanned range
λ_1	$[10^{-8}, 1]$
λ_2	$[10^{-8}, 1]$
λ_3	$\pm[10^{-8}, 1]$
λ_4	$\pm[10^{-8}, 1]$
λ_5	$\pm[10^{-8}, 1]$
m_η [GeV]	$[10, 1000]$
M_{N_1} [GeV]	$[50, 5000]$
M_{N_2} [GeV]	$[5 \times 10^3, 2 \times 10^6]$
M_{N_3} [GeV]	$[5 \times 10^3, 3.5 \times 10^6]$

Constraints.

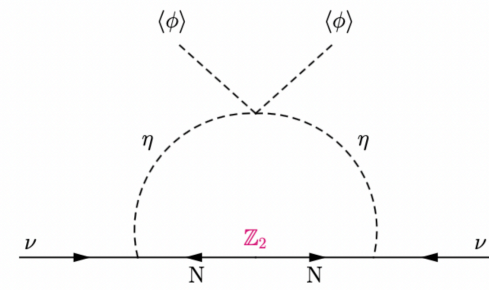
- Theoretical: η_R is the lightest (at tree level), potential bounded from below, perturbativity.
- Experimental: Neutrino masses and oscillations, electroweak precision, LFV, colliders, DM.

Neutrinos

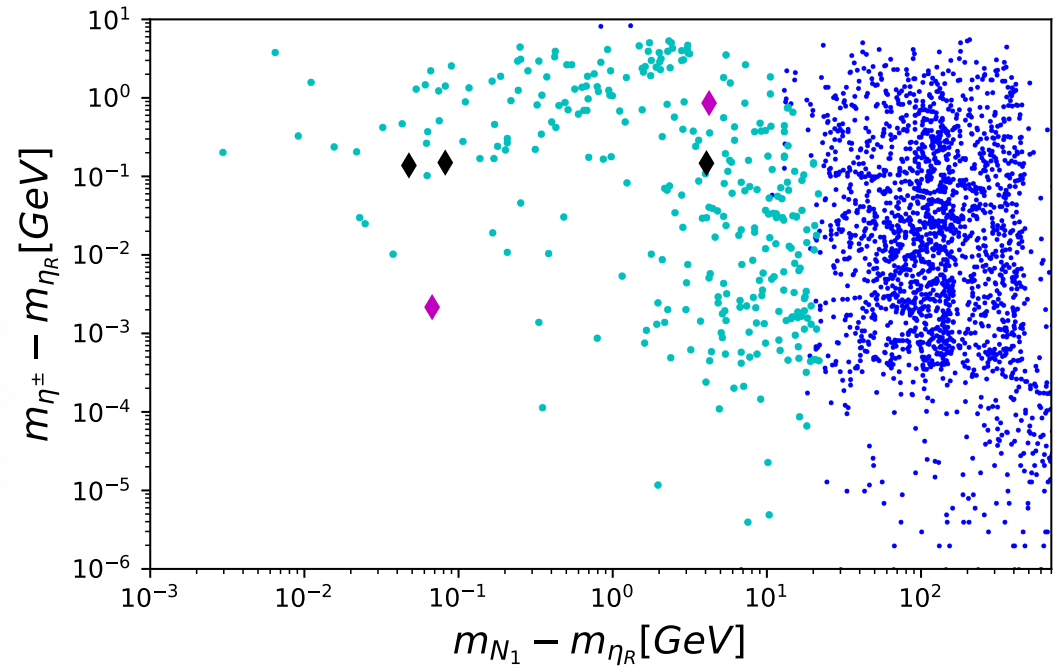
Benchmark Points

Parameter	B1	B2
λ_3	-2.809×10^{-4}	2.322×10^{-8}
λ_4	1.16×10^{-5}	-1.538×10^{-5}
λ_5	-2.511×10^{-2}	-2.878×10^{-5}
m_η^2 [GeV]	1.966×10^5	9.608×10^4
m_{η_R} [GeV]	442.535	309.961
m_{η_I} [GeV]	444.252	309.964
m_{η^\pm} [GeV]	443.394	309.964
m_{N_1} [GeV]	446.754	310.028
$c\tau_{N_1}$ [mm]	0.467	0.149
$\sigma(e^+e^- \rightarrow N_1 N_1)$ [fb]	9.89×10^{-20}	1.68×10^{-11}
Ωh^2	0.122	0.092

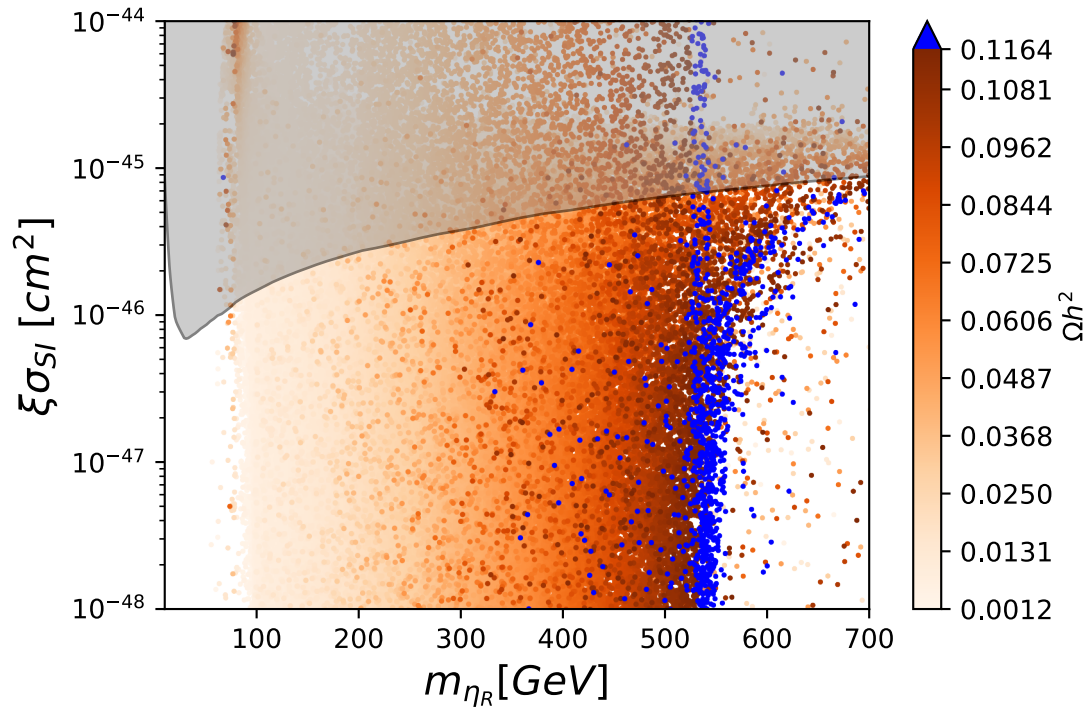
Parameter	B3	B4	B5
λ_3	-2.392×10^{-5}	3.305×10^{-6}	4.447×10^{-5}
λ_4	-6.923×10^{-7}	-1.46×10^{-3}	-3.293×10^{-6}
λ_5	-4.177×10^{-3}	-2.07×10^{-3}	-3.191×10^{-3}
m_η^2 [GeV]	1.851×10^5	1.276×10^5	1.234×10^5
m_{η_R} [GeV]	430.141	357.093	351.087
m_{η_I} [GeV]	430.435	357.269	351.362
m_{η^\pm} [GeV]	430.288	357.243	351.224
m_{N_1} [GeV]	434.197	357.175	351.134
$c\tau_{\eta^\mp}$ [mm]	16.859	14.587	28.412
$\sigma(pp \rightarrow \eta\eta j)$ [fb]	2.525	5.44	5.81
$N = \sigma \times BR \times \mathcal{L} \times \epsilon$	19.392	33.474	77.811
Ωh^2	0.121	0.121	0.119



$$\mathcal{M}_{\alpha\beta}^\nu = \frac{m_{N_i}}{32\pi^2} Y_N^{\alpha i} Y_N^{\beta i} \left[\frac{m_{\eta_R}^2}{m_{\eta_R}^2 - m_{N_i}^2} \ln\left(\frac{m_{\eta_R}^2}{m_{N_i}^2}\right) - \frac{m_{\eta_I}^2}{m_{\eta_I}^2 - m_{N_i}^2} \ln\left(\frac{m_{\eta_I}^2}{m_{N_i}^2}\right) \right]$$

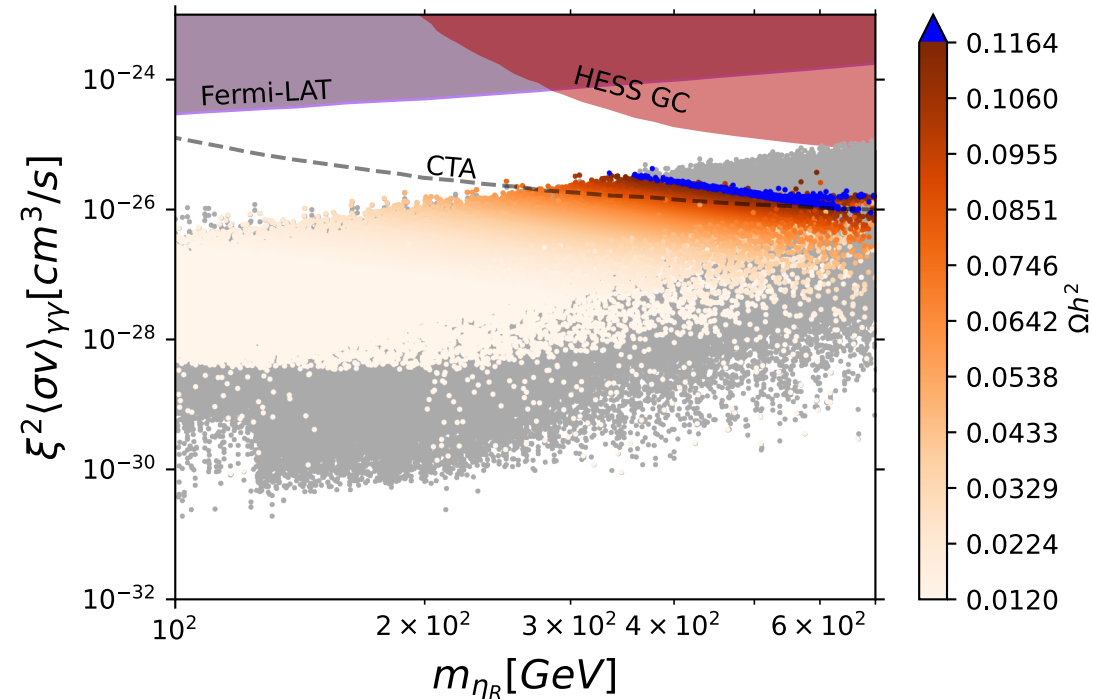


Direct and Indirect Detection



-) Indirect searches.
-) DM annihilation cross section.
-) Grey points are excluded.
-) Blue points satisfy the total relic density.
-) Orange points satisfy it partially.

-) Direct searches.
-) η_R — nucleon spin independent elastic scattering cross section.
-) Grey: XENON1T.
-) Blue points: satisfy the totality of the relic density (300 to 700 GeV).
-) Orange points satisfy it partially.

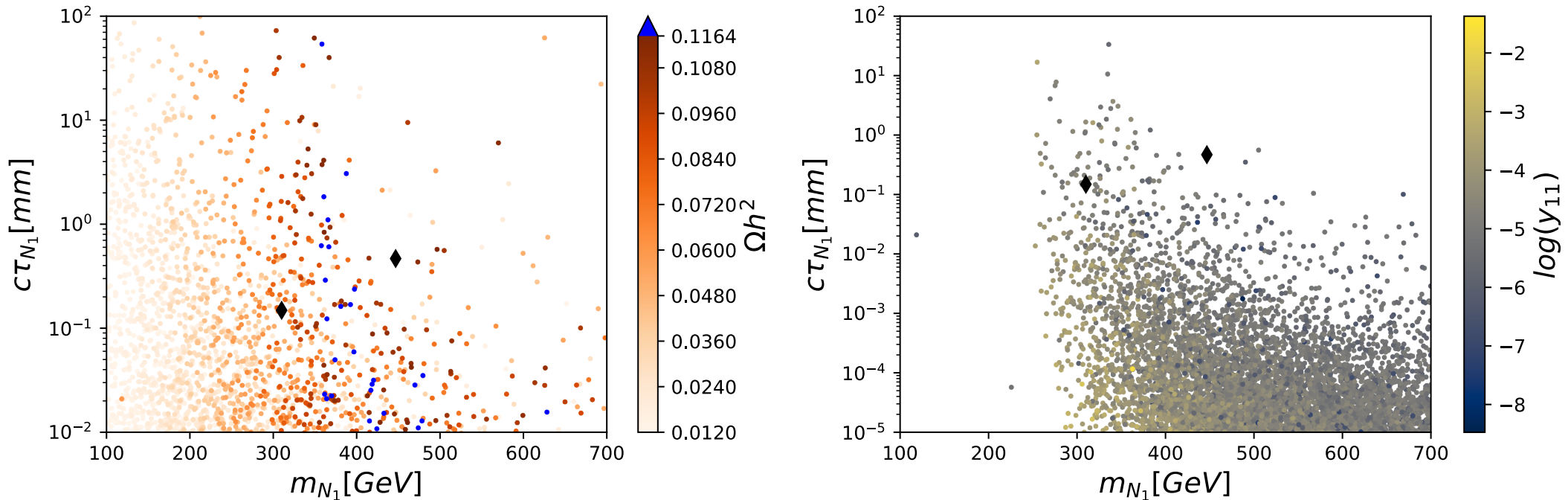


Long Lived N_1

$$\Gamma(N_k \rightarrow \ell_j^\pm \eta^\mp) = \frac{|Y_{jk}|^2}{32\pi} \frac{m_{N_k}^2 + m_{\ell_j}^2 - m_{\eta^\pm}^2}{m_{N_k}^3} \sqrt{(m_{N_k}^2 - m_{\ell_j}^2 - m_{\eta^\pm}^2)^2 - 4m_{\ell_j}^2 m_{\eta^\pm}^2}$$

$$\Gamma(N_k \rightarrow \nu \eta_\alpha) = \sum_j \frac{|Y_{jk}|^2}{32\pi} \frac{(m_{N_k}^2 - m_{\eta_\alpha}^2)^2}{m_{N_k}^3}$$

N_1 can be long-lived, but its production cross section is small.

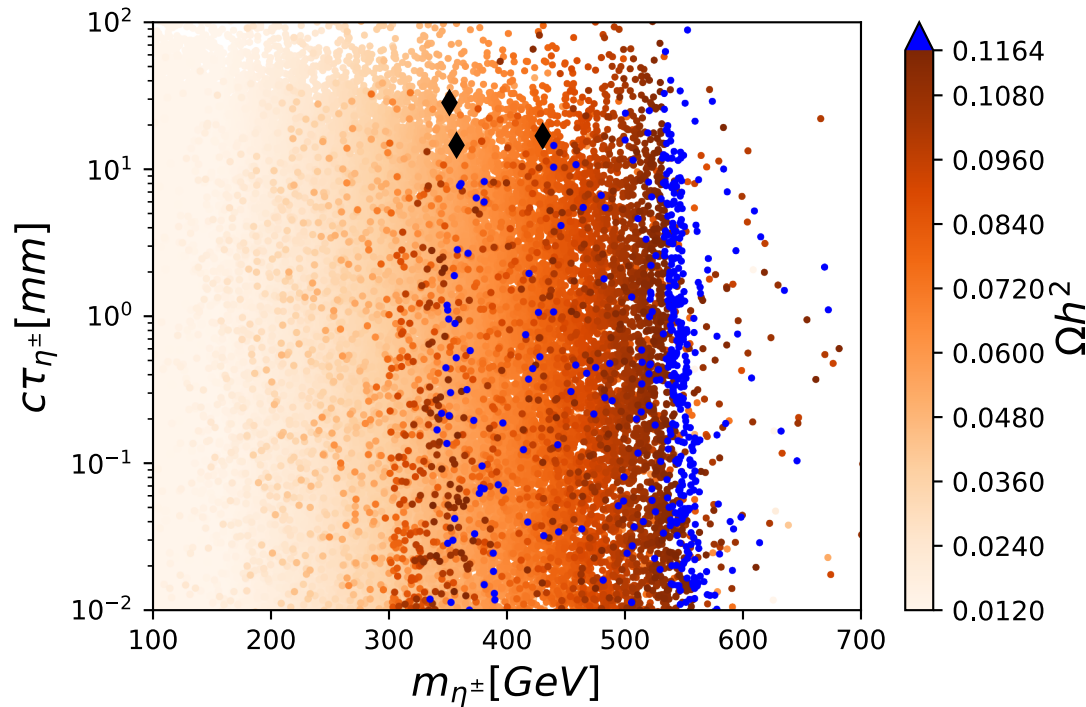


Long Lived η^\pm

$$\Gamma(\eta^\pm \rightarrow N_1 \ell^\pm) = \frac{Y_{\ell 1}^2 (m_{\eta^\pm}^2 - (m_{N_1} + m_\ell)^2)}{8\pi m_{\eta^\pm}} \sqrt{1 - \left(\frac{m_{N_1} - m_\ell}{m_{\eta^\pm}}\right)^2} \sqrt{1 - \left(\frac{m_{N_1} + m_\ell}{m_{\eta^\pm}}\right)^2}$$

$$\Gamma(\eta^\pm \rightarrow \eta_R \pi^\pm) = \frac{f_\pi^2 g^4 (m_{\eta^\pm}^2 - m_{\eta_R}^2)}{512\pi m_W^4 m_{\eta^\pm}} \sqrt{1 - \left(\frac{m_{\eta_R} - m_\pi}{m_{\eta^\pm}}\right)^2} \sqrt{1 - \left(\frac{m_{\eta_R} + m_\pi}{m_{\eta^\pm}}\right)^2}$$

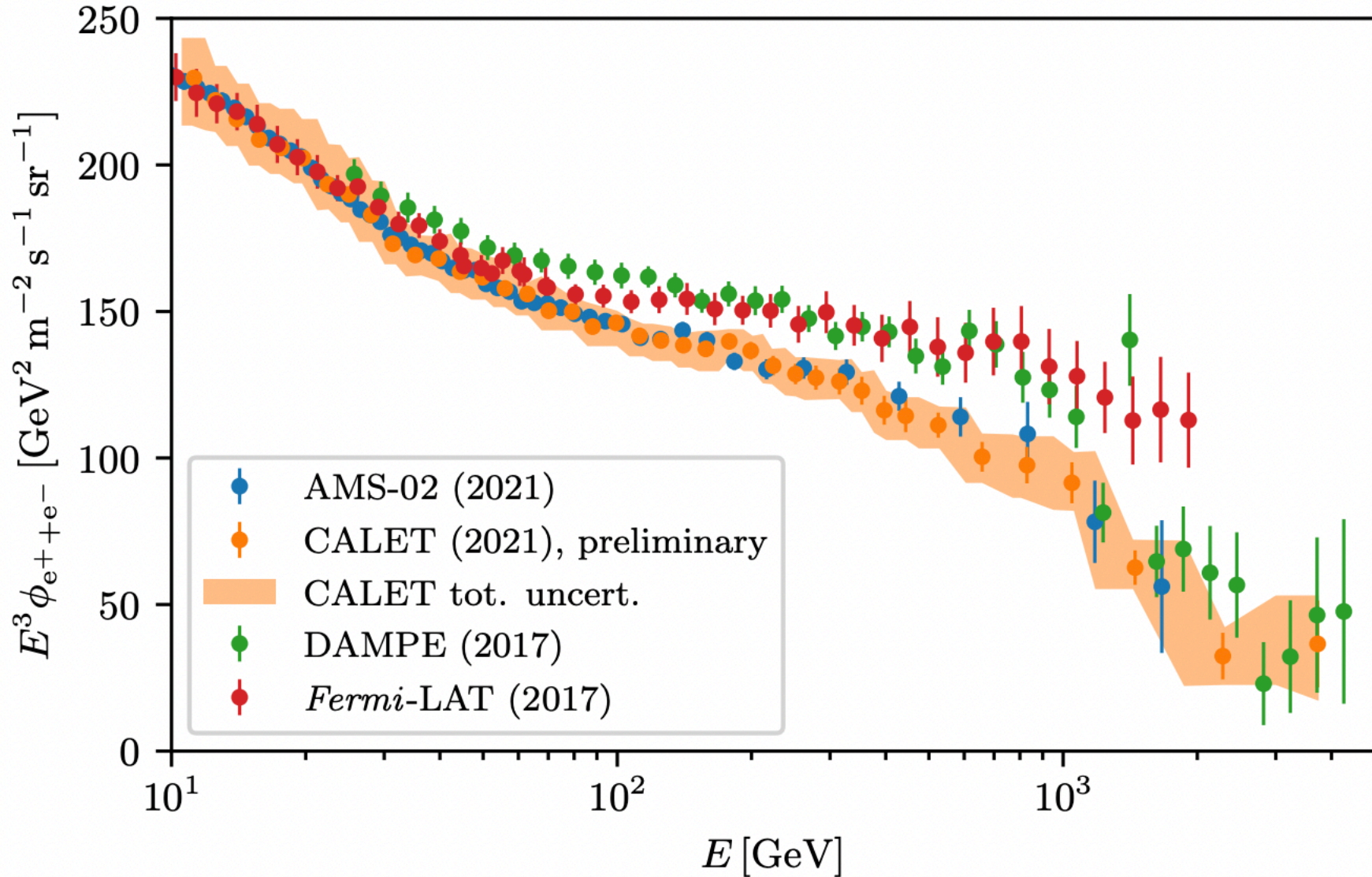
η^\pm can be long-lived, and its production cross section is large.



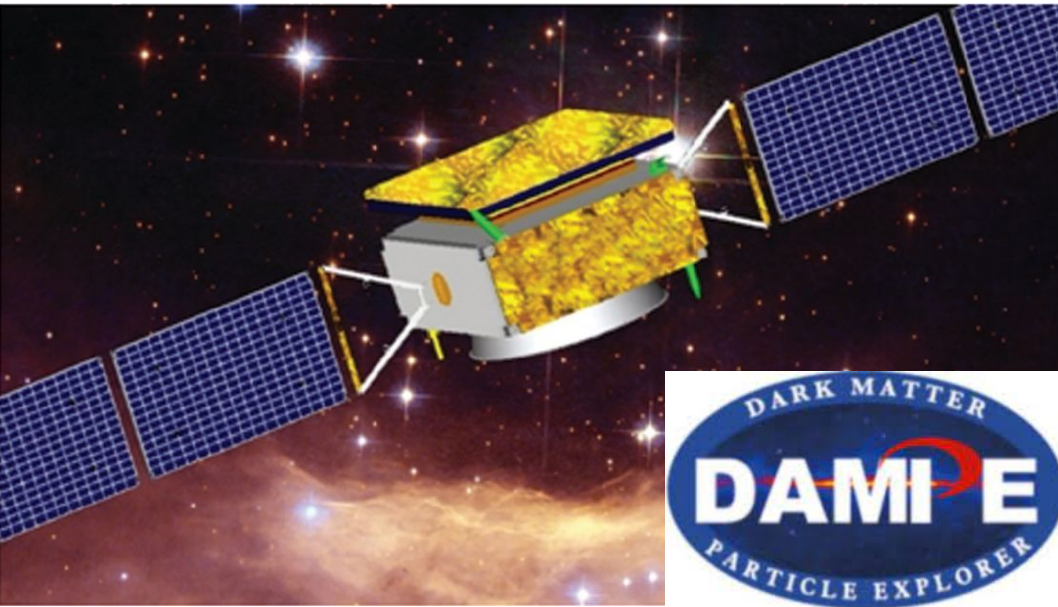
Particles from Space

All-electron Flux

Between 10 and 30 GeV: $E^{-3.25}$
Between 30 GeV and cutoff: $E^{-3.1}$ (DAMPE, Fermi-LAT)
 $E^{-3.15}$ (AMS-02, CALET)

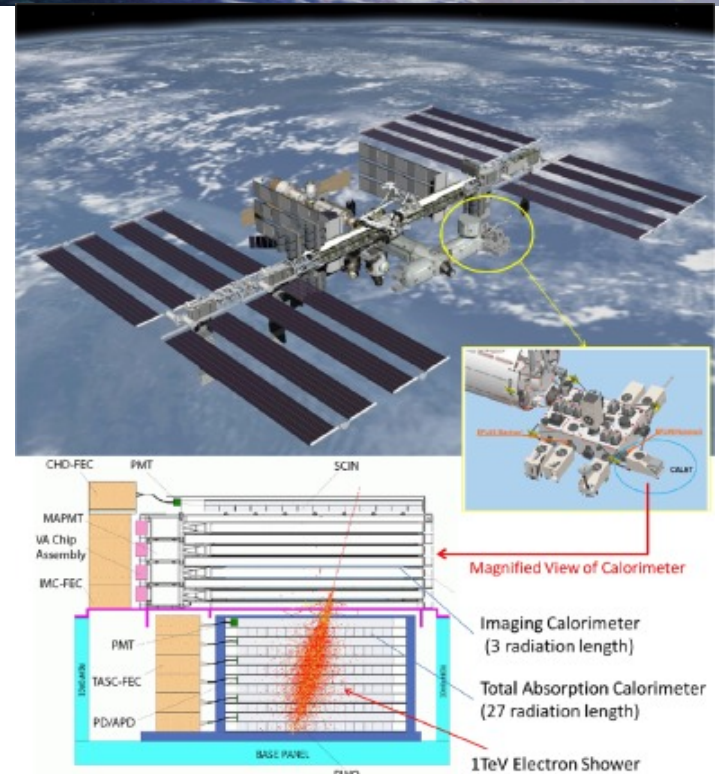
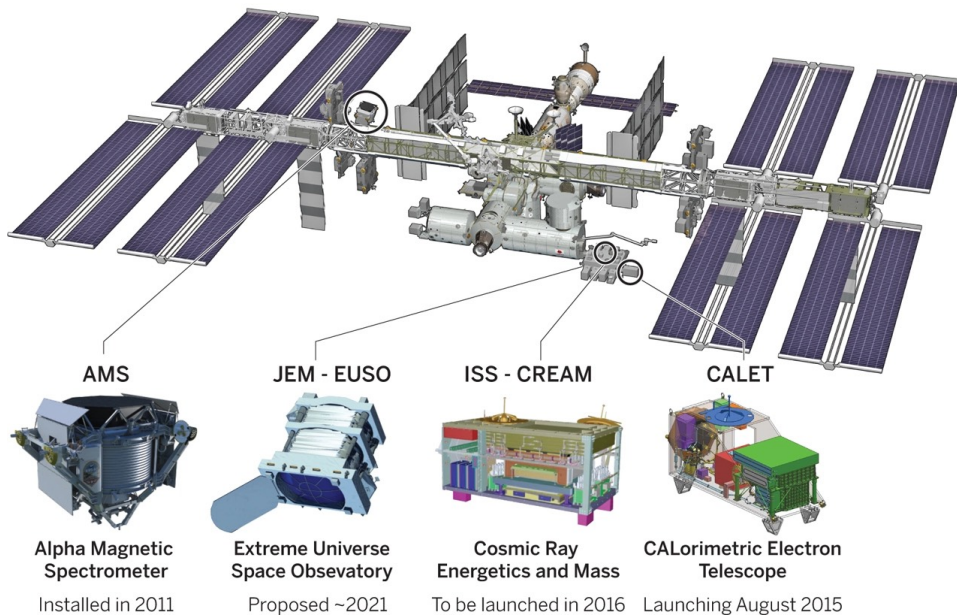


Satellites



Cosmic ray detectors on the ISS

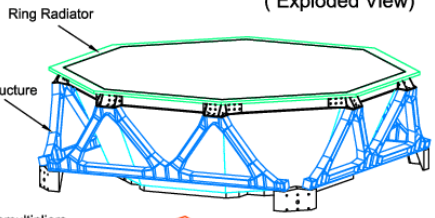
New experiments, perched outside Earth's atmosphere, promise to turn the International Space Station into a well-rounded platform for unlocking the secrets of supernovae and even dark matter.



Alpha Magnetic Spectrometer (AMS-02)



AMS 02 (Exploded View)



TRD:
Transition
Radiation
Detector

ToF: (s1,s2)
Time of Flight
Detector

TR:
Silicon Tracker

AC:
Anticoincidence
Counter

MG:
Magnet

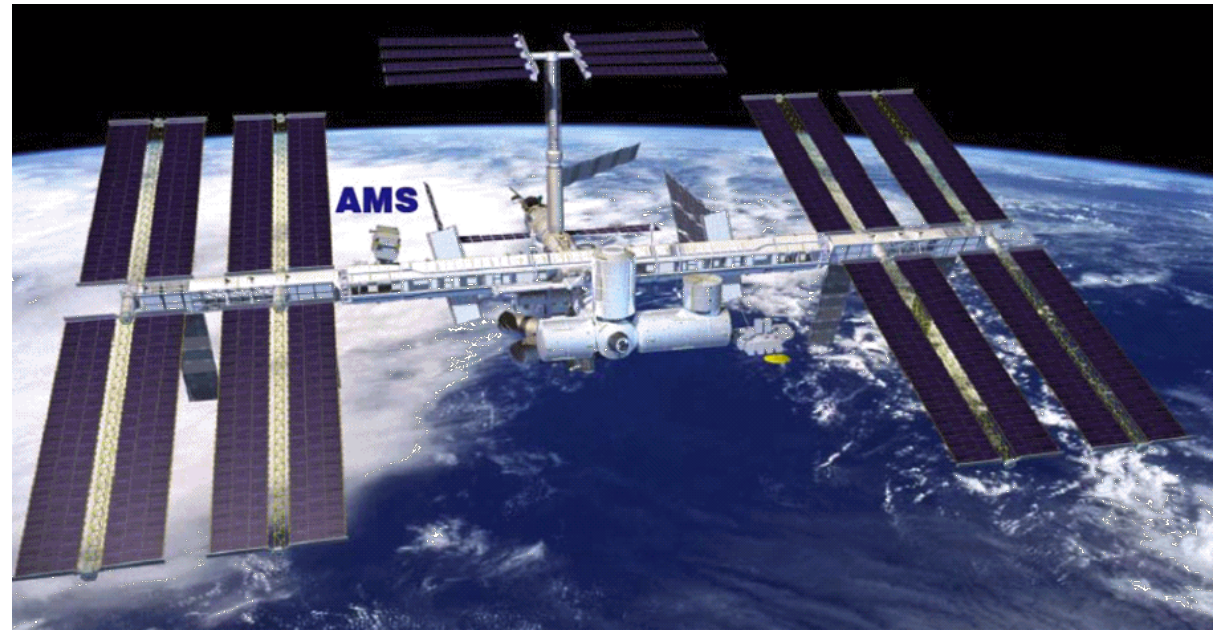
ToF: (s3,s4)
Time of Flight
Detector

RICH:
Ring image
Cherokov Counter

EMC:
Electromagnetic
Calorimeter

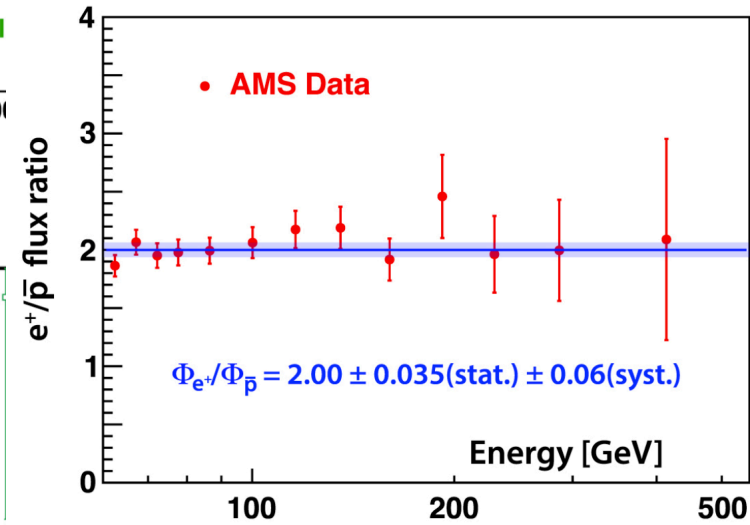
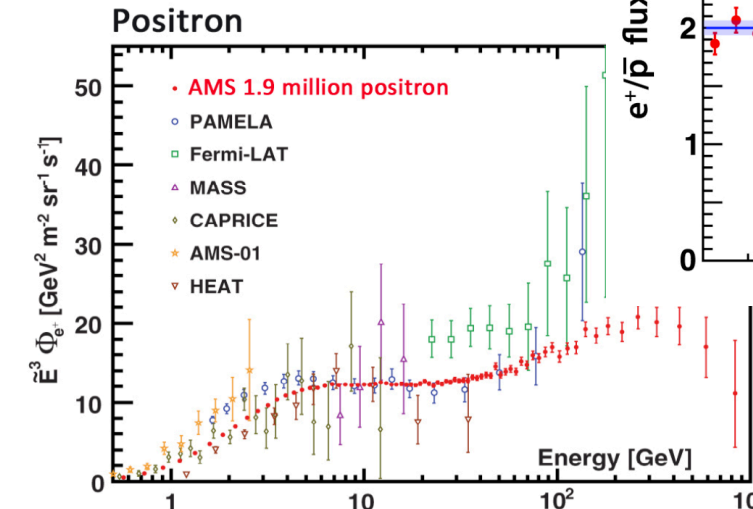
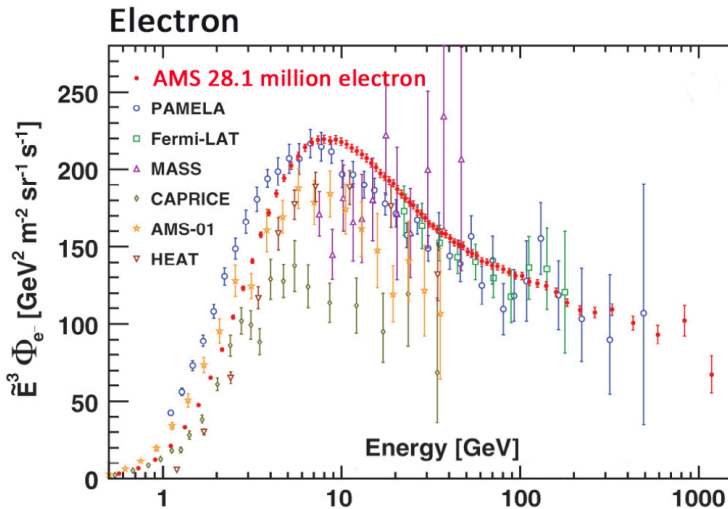
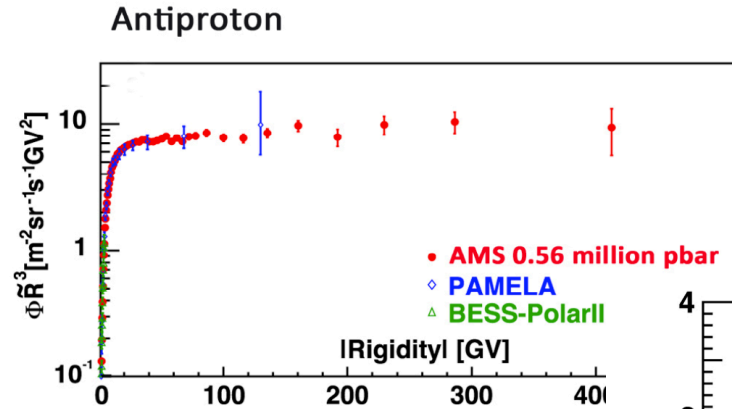
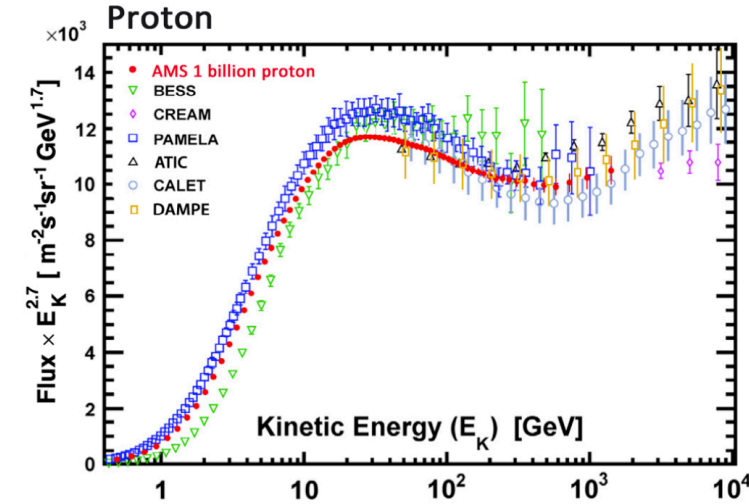
AMS Alpha
Magnetic
Spectrometer
Integration

MIT



Latest results from AMS-02

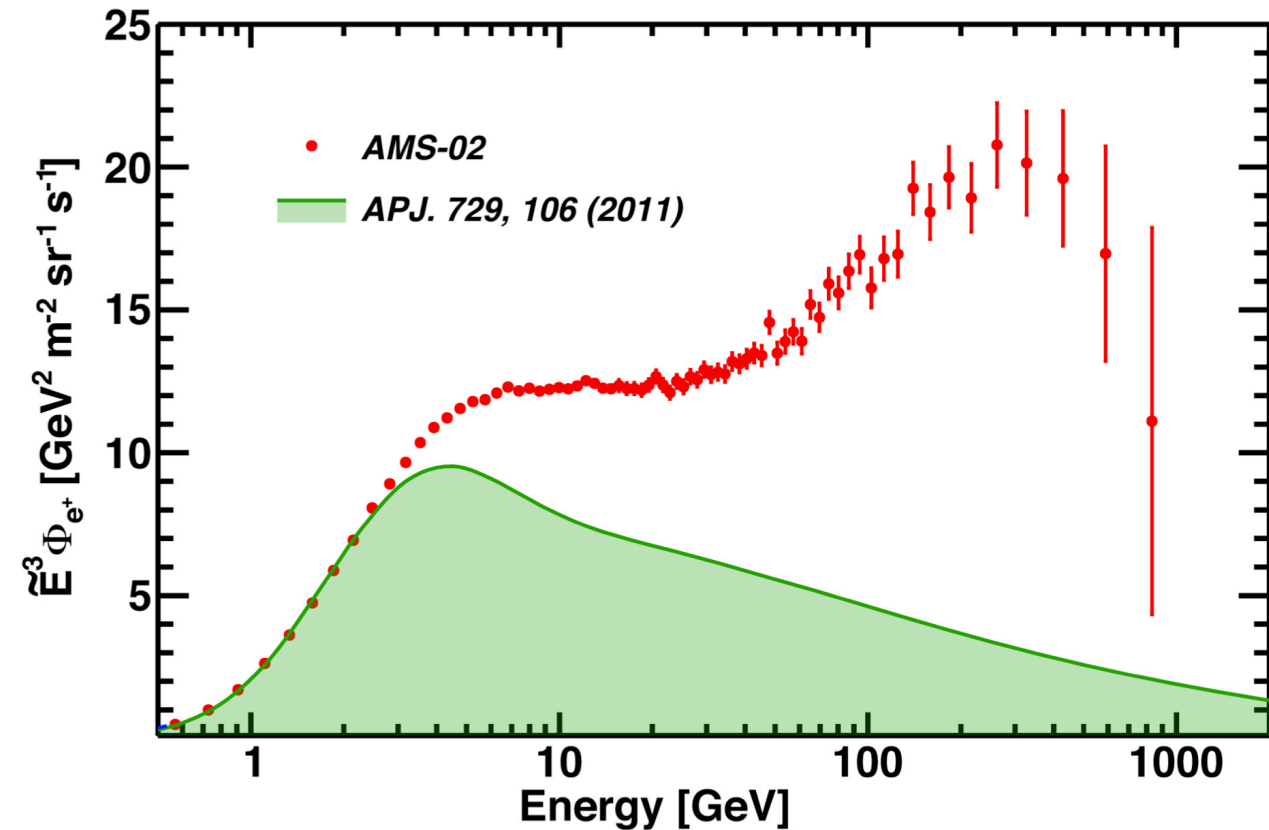
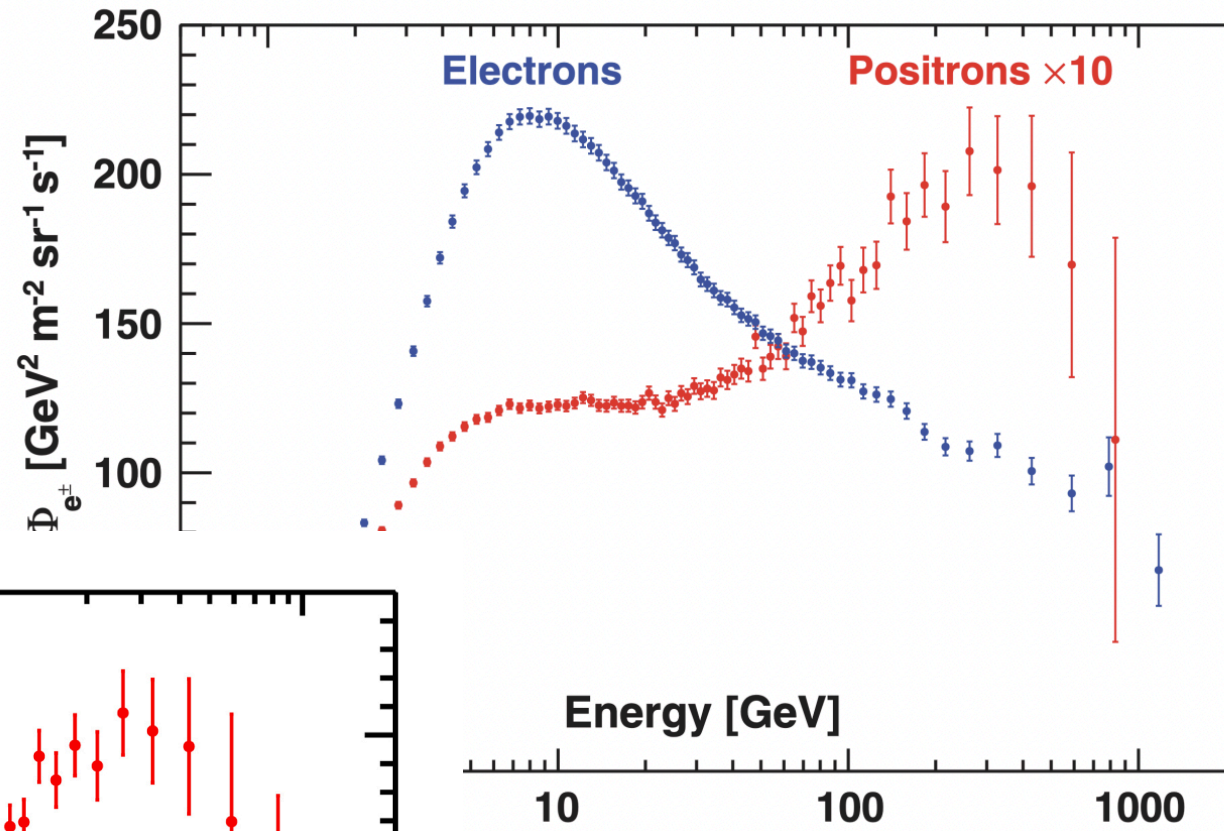
AMS-02 can differentiate between electrons and positrons, but CALET and DAMPE do not.



Significant excess starting from 25.2 ± 1.8 GeV, with a sharp drop above 284_{-64}^{+91} GeV [Z. Weng, PoS 045, ICHEP2020 (2020)]. Antiproton flux has a similar behavior.

Latest Results on Electrons and Positrons from AMS

Rise on positron flux persists withtime [Z. Weng, PoS 045, ICHEP2020 (2020)].



Positron flux measured by AMS-02 [J. Bedugo, PoS 016, ICRC2021 (2021)] compared to GALPROP prediction for cosmic rays.

Supersymmetry

1.- R-Parity (Rp) Conserving:

a.- Dark Matter (DM) candidate: neutralino

b.- Superpotential:

$$W_{MSSM} = (\mu \hat{H}_u^a \hat{H}_d^b + h_{ij}^e \hat{H}_d^a \hat{H}_u^b + h_{ij}^d \hat{H}_d^a \hat{Q}_i^b \hat{D}_j - h_{ij}^u \hat{H}_u^a \hat{Q}_i^b \hat{U}_j) \epsilon_{ab}$$

2.- R-Parity Violating:

a.- Dark Matter candidate: gravitino

b.- Superpotential:

$$W_{MSSM+RpV} = W_{MSSM} + (\epsilon_i \hat{H}_u^a \hat{L}_i^b + \frac{1}{2} \lambda_{ijk} \hat{L}_i^a \hat{L}_j^b \hat{R}_k + \lambda'_{ijk} \hat{L}_i^a \hat{Q}_j^b \hat{D}_k) \epsilon_{ab} + \frac{1}{2} \lambda''_{ijk} \hat{U}_i \hat{D}_j \hat{D}_k$$

3.- The gravitino interaction is governed by:

$$\mathcal{L} = -\frac{1}{\sqrt{2}M_P} \bar{F} \gamma^\mu \gamma^\nu \partial_\nu \tilde{F} \tilde{G}_\mu$$

Latest Results for ATLAS Susy Searches

ATLAS SUSY Searches* - 95% CL Lower Limits

March 2022

ATLAS Preliminary

$\sqrt{s} = 13$ TeV

Model	Signature	$\int \mathcal{L} dt$ [fb $^{-1}$]	Mass limit	Reference						
Inclusive Searches	$\tilde{q}\tilde{q}, \tilde{q} \rightarrow q\tilde{\chi}_1^0$	0 e, μ mono-jet	2-6 jets 1-3 jets	E_{T}^{miss} E_{T}^{miss}	139 139	\tilde{q} [1x, 8x Degen.] \tilde{q} [8x Degen.]	1.0 0.9	1.85	$m(\tilde{\chi}_1^0) < 400$ GeV $m(\tilde{q}) - m(\tilde{\chi}_1^0) = 5$ GeV	2101.14293 2102.10874
	$\tilde{g}\tilde{g}, \tilde{g} \rightarrow q\tilde{q}\tilde{\chi}_1^0$	0 e, μ	2-6 jets	E_{T}^{miss}	139	\tilde{g} \tilde{g}	2.3	1.15-1.95	$m(\tilde{\chi}_1^0) = 0$ GeV $m(\tilde{\chi}_1^0) = 1000$ GeV	2101.14293 2101.14293
	$\tilde{g}\tilde{g}, \tilde{g} \rightarrow q\tilde{q}W\tilde{\chi}_1^0$	1 e, μ	2-6 jets	E_{T}^{miss}	139	\tilde{g}	2.2	2.2	$m(\tilde{\chi}_1^0) < 600$ GeV $m(\tilde{\chi}_1^0) < 700$ GeV	2101.01629 CERN-EP-2022-014
	$\tilde{g}\tilde{g}, \tilde{g} \rightarrow q\tilde{q}(\ell)\tilde{\chi}_1^0$	0 e, μ	7-11 jets	E_{T}^{miss}	139	\tilde{g}	1.97	1.15	$m(\tilde{\chi}_1^0) < 600$ GeV $m(\tilde{g}) - m(\tilde{\chi}_1^0) = 200$ GeV	2008.06032 1909.08457
	$\tilde{g}\tilde{g}, \tilde{g} \rightarrow q\tilde{q}WZ\tilde{\chi}_1^0$	SS e, μ	6 jets	E_{T}^{miss}	139	\tilde{g}	1.25	2.25	$m(\tilde{\chi}_1^0) < 200$ GeV $m(\tilde{g}) - m(\tilde{\chi}_1^0) = 300$ GeV	ATLAS-CONF-2018-041 1909.08457
	$\tilde{g}\tilde{g}, \tilde{g} \rightarrow t\tilde{\chi}_1^0$	0-1 e, μ SS e, μ	3 b 6 jets	E_{T}^{miss}	79.8 139	\tilde{g} \tilde{g}	1.25	2.25	$m(\tilde{\chi}_1^0) < 200$ GeV $m(\tilde{g}) - m(\tilde{\chi}_1^0) = 300$ GeV	ATLAS-CONF-2018-041 1909.08457
	$\tilde{b}_1\tilde{b}_1$	0 e, μ	2 b	E_{T}^{miss}	139	\tilde{b}_1 \tilde{b}_1	0.68	1.255	$m(\tilde{\chi}_1^0) < 400$ GeV 10 GeV $< \Delta m(\tilde{b}_1, \tilde{\chi}_1^0) < 20$ GeV	2101.12527 2101.12527
3 rd gen. squarks direct production	$\tilde{b}_1\tilde{b}_1, \tilde{b}_1 \rightarrow b\tilde{\chi}_2^0 \rightarrow b\tilde{h}\tilde{\chi}_1^0$	0 e, μ 2 τ	6 b 2 b	E_{T}^{miss} E_{T}^{miss}	139 139	\tilde{b}_1 \tilde{b}_1	Forbidden	0.23-1.35	$\Delta m(\tilde{\chi}_2^0, \tilde{\chi}_1^0) = 130$ GeV, $m(\tilde{\chi}_1^0) = 100$ GeV $\Delta m(\tilde{\chi}_2^0, \tilde{\chi}_1^0) = 130$ GeV, $m(\tilde{\chi}_1^0) = 0$ GeV	1908.03122 2103.08189
	$\tilde{t}_1\tilde{t}_1, \tilde{t}_1 \rightarrow t\tilde{\chi}_1^0$	0-1 e, μ	≥ 1 jet	E_{T}^{miss}	139	\tilde{t}_1	1.25	1.25	$m(\tilde{\chi}_1^0) = 1$ GeV	2004.14060, 2012.03799
	$\tilde{t}_1\tilde{t}_1, \tilde{t}_1 \rightarrow Wb\tilde{\chi}_1^0$	1 e, μ	3 jets/1 b	E_{T}^{miss}	139	\tilde{t}_1	0.65	Forbidden	$m(\tilde{\chi}_1^0) = 500$ GeV	2012.03799
	$\tilde{t}_1\tilde{t}_1, \tilde{t}_1 \rightarrow \tilde{\tau}b\nu, \tilde{\tau}_1 \rightarrow \tau\tilde{G}$	1-2 τ	2 jets/1 b	E_{T}^{miss}	139	\tilde{t}_1	1.4	Forbidden	$m(\tilde{\tau}_1) = 800$ GeV	2108.07665
	$\tilde{t}_1\tilde{t}_1, \tilde{t}_1 \rightarrow c\tilde{\chi}_1^0 / \tilde{c}\tilde{c}, \tilde{c} \rightarrow c\tilde{\chi}_1^0$	0 e, μ 0 e, μ	2 c mono-jet	E_{T}^{miss} E_{T}^{miss}	36.1 139	\tilde{c} \tilde{t}_1	0.55	0.85	$m(\tilde{\chi}_1^0) = 0$ GeV $m(\tilde{t}_1, \tilde{c}) - m(\tilde{\chi}_1^0) = 5$ GeV	1805.01649 2102.10874
	$\tilde{t}_1\tilde{t}_1, \tilde{t}_1 \rightarrow t\tilde{\chi}_2^0, \tilde{\chi}_2^0 \rightarrow Z/h\tilde{\chi}_1^0$	1-2 e, μ	1-4 b	E_{T}^{miss}	139	\tilde{t}_1	0.067-1.18	0.86	$m(\tilde{\chi}_2^0) = 500$ GeV $m(\tilde{t}_1) = 360$ GeV, $m(\tilde{t}_1) - m(\tilde{\chi}_1^0) = 40$ GeV	2006.05880 2006.05880
	$\tilde{t}_2\tilde{t}_2, \tilde{t}_2 \rightarrow \tilde{t}_1 + Z$	3 e, μ	1 b	E_{T}^{miss}	139	\tilde{t}_2	Forbidden	0.86		
EW direct	$\tilde{\chi}_1^{\pm}\tilde{\chi}_2^0$ via WZ	Multiple ℓ/jets $ee, \mu\mu$	≥ 1 jet	E_{T}^{miss} E_{T}^{miss}	139 139	$\tilde{\chi}_1^{\pm}/\tilde{\chi}_2^0$ $\tilde{\chi}_1^{\pm}/\tilde{\chi}_2^0$	0.205	0.96	$m(\tilde{\chi}_1^0) = 0$, wino-bino $m(\tilde{\chi}_1^{\pm}) - m(\tilde{\chi}_1^0) = 5$ GeV, wino-bino	2106.01676, 2108.07586 1911.12606
	$\tilde{\chi}_1^{\pm}\tilde{\chi}_1^{\mp}$ via WW	2 e, μ		E_{T}^{miss}	139	$\tilde{\chi}_1^{\pm}$	0.42	1.06	$m(\tilde{\chi}_1^0) = 0$, wino-bino	1908.08215
	$\tilde{\chi}_1^{\pm}\tilde{\chi}_2^0$ via Wh	Multiple ℓ/jets		E_{T}^{miss}	139	$\tilde{\chi}_1^{\pm}/\tilde{\chi}_2^0$	Forbidden	1.0	$m(\tilde{\chi}_1^0) = 70$ GeV, wino-bino	2004.10894, 2108.07586
	$\tilde{\chi}_1^{\pm}\tilde{\chi}_1^{\mp}$ via $\tilde{\ell}_L/\tilde{\nu}$	2 e, μ		E_{T}^{miss}	139	$\tilde{\chi}_1^{\pm}$	1.0	1.0	$m(\tilde{\ell}, \tilde{\nu}) = 0.5(m(\tilde{\chi}_1^{\pm}) + m(\tilde{\chi}_1^0))$	1908.08215
	$\tilde{\tau}\tilde{\tau}, \tilde{\tau} \rightarrow \tau\tilde{\chi}_1^0$	2 τ		E_{T}^{miss}	139	$\tilde{\tau}$	0.16-0.3	0.12-0.39	$m(\tilde{\chi}_1^0) = 0$	1911.06660
	$\tilde{\ell}_{L,R}\tilde{\ell}_{L,R}, \tilde{\ell} \rightarrow \ell\tilde{\chi}_1^0$	2 e, μ $ee, \mu\mu$	0 jets ≥ 1 jet	E_{T}^{miss} E_{T}^{miss}	139 139	$\tilde{\ell}$ $\tilde{\ell}$	0.256	0.7	$m(\tilde{\chi}_1^0) = 0$ $m(\tilde{\ell}) - m(\tilde{\chi}_1^0) = 10$ GeV	1908.08215 1911.12606
	$\tilde{H}\tilde{H}, \tilde{H} \rightarrow h\tilde{G}/Z\tilde{G}$	0 e, μ 4 e, μ 0 e, μ	≥ 3 b 0 jets ≥ 2 large jets	E_{T}^{miss} E_{T}^{miss} E_{T}^{miss}	36.1 139 139	\tilde{H} \tilde{H} \tilde{H}	0.13-0.23	0.29-0.88	$\text{BR}(\tilde{\chi}_1^0 \rightarrow h\tilde{G}) = 1$ $\text{BR}(\tilde{\chi}_1^0 \rightarrow Z\tilde{G}) = 1$ $\text{BR}(\tilde{\chi}_1^0 \rightarrow \tilde{G}) = 1$	1806.04030 2103.11684 2108.07586
Long-lived particles	Direct $\tilde{\chi}_1^{\pm}\tilde{\chi}_1^{\mp}$ prod., long-lived $\tilde{\chi}_1^{\pm}$	Disapp. trk	1 jet	E_{T}^{miss}	139	$\tilde{\chi}_1^{\pm}$ $\tilde{\chi}_1^{\pm}$	0.66	0.21	Pure Wino Pure higgsino	2201.02472 2201.02472
	Stable \tilde{g} R-hadron	pixel dE/dx		E_{T}^{miss}	139	\tilde{g}	2.05			CERN-EP-2022-029
	Metastable \tilde{g} R-hadron, $\tilde{g} \rightarrow q\tilde{q}\tilde{\chi}_1^0$	pixel dE/dx		E_{T}^{miss}	139	\tilde{g}	[$\tau(\tilde{g}) = 10$ ns]	2.2	$m(\tilde{\chi}_1^0) = 100$ GeV	CERN-EP-2022-029
	$\tilde{\ell}\tilde{\ell}, \tilde{\ell} \rightarrow \ell\tilde{G}$	Displ. lep		E_{T}^{miss}	139	$\tilde{e}, \tilde{\mu}$ $\tilde{\tau}$ $\tilde{\tau}$	0.34 0.36	0.7	$\tau(\tilde{\ell}) = 0.1$ ns $\tau(\tilde{\ell}) = 0.1$ ns $\tau(\tilde{\ell}) = 10$ ns	2011.07812 2011.07812 CERN-EP-2022-029
RPV	$\tilde{\chi}_1^{\pm}\tilde{\chi}_1^{\mp}/\tilde{\chi}_1^0, \tilde{\chi}_1^{\pm} \rightarrow Z\ell + \ell\ell\ell$	3 e, μ		E_{T}^{miss}	139	$\tilde{\chi}_1^{\pm}/\tilde{\chi}_1^0$ [BR(Z τ)=1, BR(Z e)=1]	0.625	1.05	Pure Wino	2011.10543
	$\tilde{\chi}_1^{\pm}\tilde{\chi}_1^{\mp}/\tilde{\chi}_2^0 \rightarrow WW/Z\ell\ell\ell\nu\nu$	4 e, μ	0 jets	E_{T}^{miss}	139	$\tilde{\chi}_1^{\pm}/\tilde{\chi}_2^0$ [$\lambda_{133} \neq 0, \lambda_{124} \neq 0$]	0.95	1.55	$m(\tilde{\chi}_1^0) = 200$ GeV	2103.11684
	$\tilde{g}\tilde{g}, \tilde{g} \rightarrow q\tilde{q}\tilde{\chi}_1^0, \tilde{\chi}_1^0 \rightarrow q\tilde{q}q$	4-5 large jets		E_{T}^{miss}	36.1	\tilde{g} [$m(\tilde{\chi}_1^0) = 200$ GeV, 1100 GeV]	1.3	1.9	Large λ'_{112}	1804.03568
	$\tilde{u}, \tilde{t} \rightarrow \tilde{\chi}_1^0, \tilde{\chi}_1^0 \rightarrow t\tilde{b}s$	Multiple		E_{T}^{miss}	36.1	\tilde{t} [$\lambda'_{234} = 2e-4, 1e-2$]	0.55	1.05	$m(\tilde{\chi}_1^0) = 200$ GeV, bino-like	ATLAS-CONF-2018-003
	$\tilde{u}, \tilde{t} \rightarrow b\tilde{\chi}_1^+, \tilde{\chi}_1^+ \rightarrow b\tilde{s}$	≥ 4 b		E_{T}^{miss}	139	\tilde{t}	Forbidden	0.95	$m(\tilde{\chi}_1^0) = 500$ GeV	2010.01015
	$\tilde{t}_1\tilde{t}_1, \tilde{t}_1 \rightarrow b\tilde{s}$	2 jets + 2 b		E_{T}^{miss}	36.7	\tilde{t}_1 [qq, bs]	0.42	0.61		1710.07171
	$\tilde{t}_1\tilde{t}_1, \tilde{t}_1 \rightarrow q\tilde{\ell}$	2 e, μ 1 μ	2 b DV	E_{T}^{miss}	36.1 136	\tilde{t}_1 \tilde{t}_1	1.0	0.4-1.45	$\text{BR}(\tilde{t}_1 \rightarrow b\tilde{c}/h\mu) > 20\%$ $\text{BR}(\tilde{t}_1 \rightarrow q\mu) = 100\%$, $\cos\theta_t = 1$	1710.05544 2003.11956
$\tilde{\chi}_1^{\pm}/\tilde{\chi}_2^0/\tilde{\chi}_1^0, \tilde{\chi}_1^0 \rightarrow t\tilde{b}s, \tilde{\chi}_1^0 \rightarrow b\tilde{b}s$	1-2 e, μ	≥ 6 jets	E_{T}^{miss}	139	$\tilde{\chi}_1^0$	0.2-0.32		Pure higgsino	2106.09609	

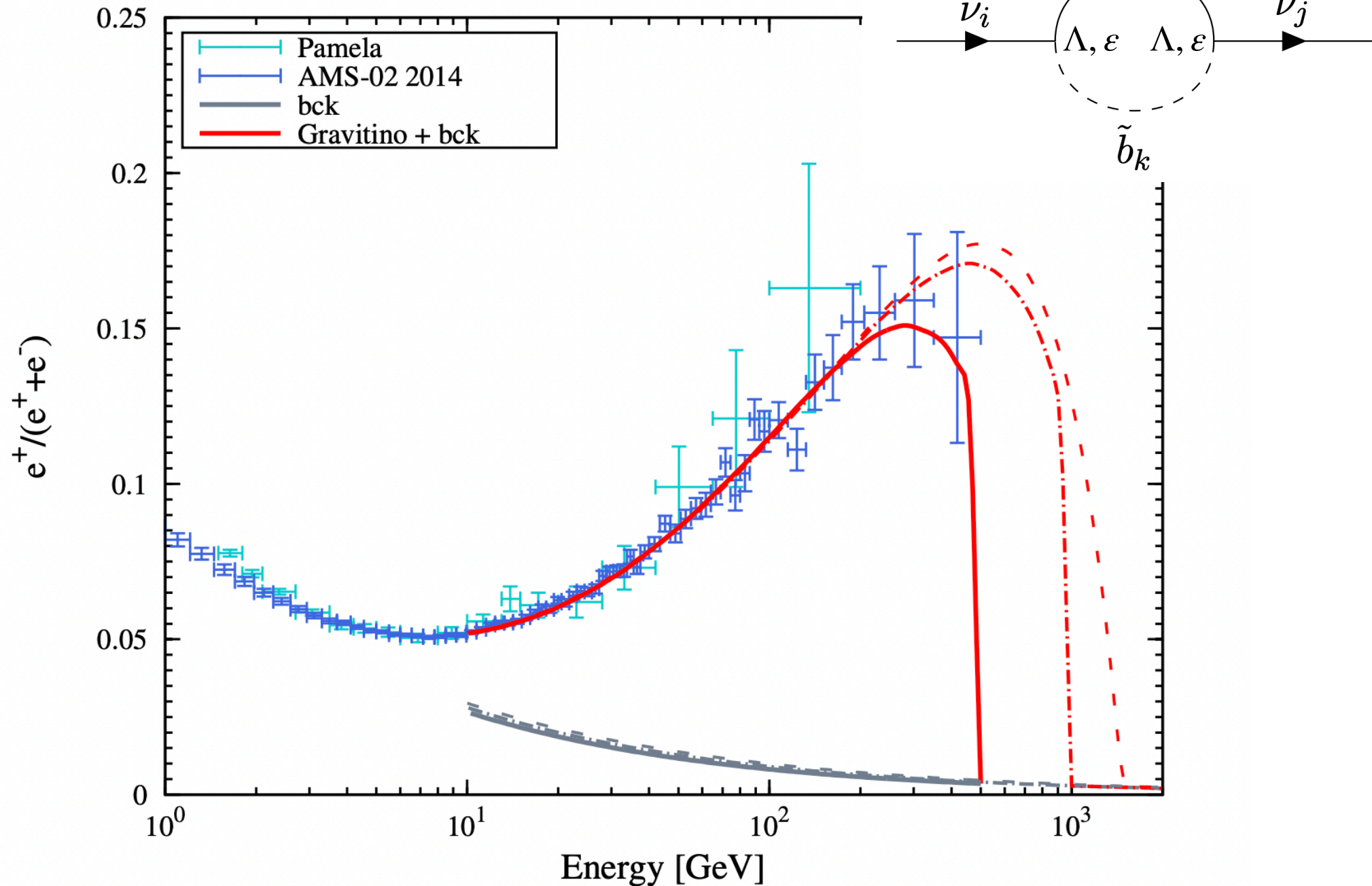
*Only a selection of the available mass limits on new states or phenomena is shown. Many of the limits are based on simplified models, c.f. refs. for the assumptions made.

10⁻¹

1

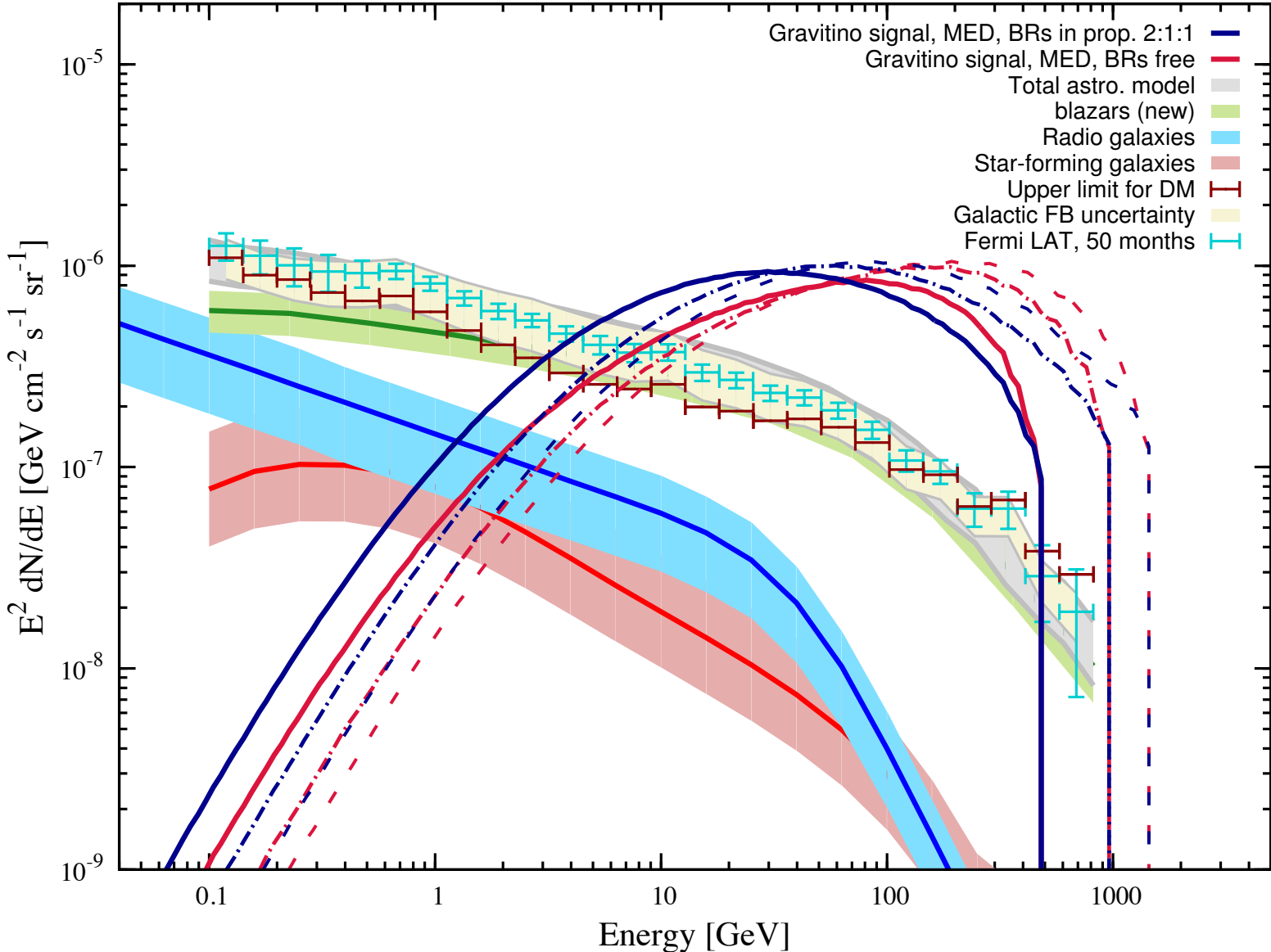
Mass scale [TeV]

BRpV Only

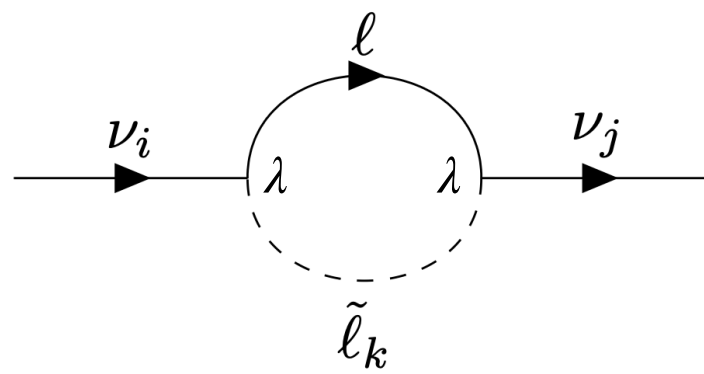


Based on *Phys. Dark Univ.* **11**, 1 (2016), in collaboration with E. Carquin, G. Gómez-Vargas, B. Panes, and N. Viaux.

Explains the rise and drop of the positrons flux, but emits too many photons. That is, the galaxy would be too bright.



TRpV Only



$$\Phi_{e^-} = C_e \left(\frac{E}{1 \text{ GeV}} \right)^{-\gamma_e}$$

$$\Phi_{e^+} = C_p \left(\frac{E}{1 \text{ GeV}} \right)^{-\gamma_p}$$

$$\alpha_1 = B(\tilde{G} \rightarrow e^- e^+ \nu) + B(\tilde{G} \rightarrow e^- \mu^+ \nu) + B(\tilde{G} \rightarrow e^- \tau^+ \nu)$$

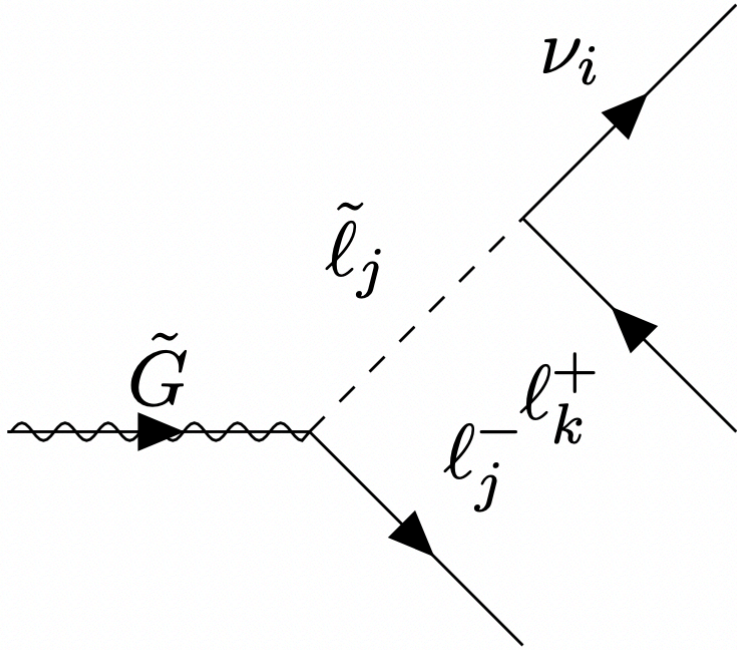
$$\alpha_2 = B(\tilde{G} \rightarrow \mu^- e^+ \nu) + B(\tilde{G} \rightarrow \mu^- \mu^+ \nu) + B(\tilde{G} \rightarrow \mu^- \tau^+ \nu)$$

$$\alpha_3 = B(\tilde{G} \rightarrow \tau^- e^+ \nu) + B(\tilde{G} \rightarrow \tau^- \mu^+ \nu) + B(\tilde{G} \rightarrow \tau^- \tau^+ \nu)$$

Parameter	Case 1	Case 2	Case 3	Case 4
C_p [1/GeV cm ² s str]	14.90	14.74	14.93	14.37
γ_p	3.11	3.10	3.11	3.09
C_e [1/GeV cm ² s str]	426.10	421.77	422.08	422.67
γ_e	3.27	3.27	3.27	3.27
m_G [GeV]	1281	2274	3604	3751
τ_G [10 ²⁶ s]	4.61	3.59	2.27	2.29
$\alpha_1 : e^- l^+ \nu$	0.43	0.06	0.03	0.32
$\alpha_2 : \mu^- l^+ \nu$	0.03	0.36	0.15	0
$\alpha_3 : \tau^- l^+ \nu$	0.54	0.58	0.82	0.68

Based on *e-Print 2011.09344*, in collaboration with J. Buchner, E. Carquin, G. Gómez-Vargas, B. Panes, and N. Viaux.

Gravitino decay



$$\tilde{m} \equiv m_{\tilde{\nu}_i} = m_{\tilde{\ell}_{i,1}} = m_{\tilde{\ell}_{i,2}}$$

$$\Gamma(\tilde{G} \rightarrow \nu_i e_j \bar{e}_k) \approx \frac{\lambda_{ijk}^2}{3\pi^3 2^{11}} \frac{m_{\tilde{G}}^7}{M_{\text{P}}^2 \tilde{m}^4}$$

$$\tau_{\tilde{G}} = 4 \times 10^{26} \text{ s} \left(\frac{1}{\lambda_{ijk} \lambda_{ijk}} \right) \left(\frac{\tilde{m}}{10^8 \text{ GeV}} \right)^4 \left(\frac{2 \text{ TeV}}{m_{\tilde{G}}} \right)^7$$

Neutrinos

$$M_{ij}^{\nu(1)} \approx \frac{1}{16\pi^2} \sum_{gr} s_{\tilde{\ell}} c_{\tilde{\ell}} (\lambda_{igr} \lambda_{jrg} + \lambda_{jgr} \lambda_{irg}) m_g \ln \frac{m_{\tilde{\ell}_{r,2}}^2}{m_{\tilde{\ell}_{r,1}}^2}$$

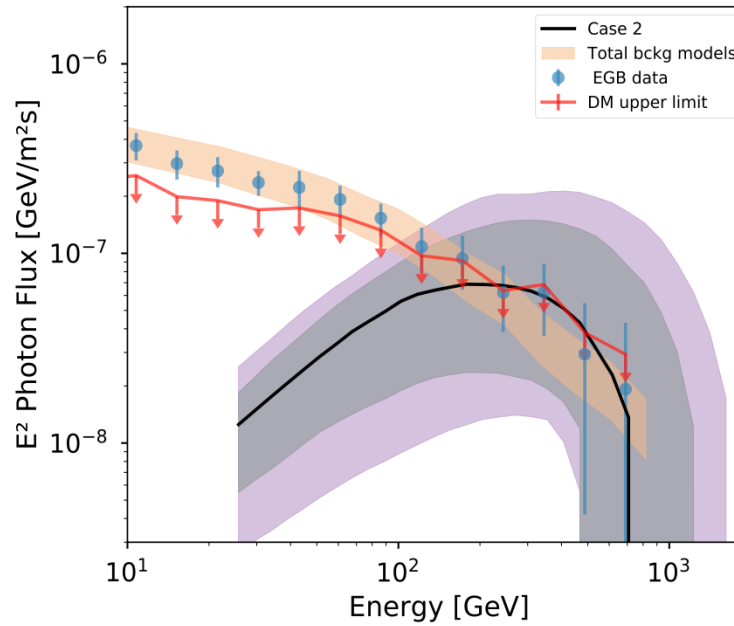
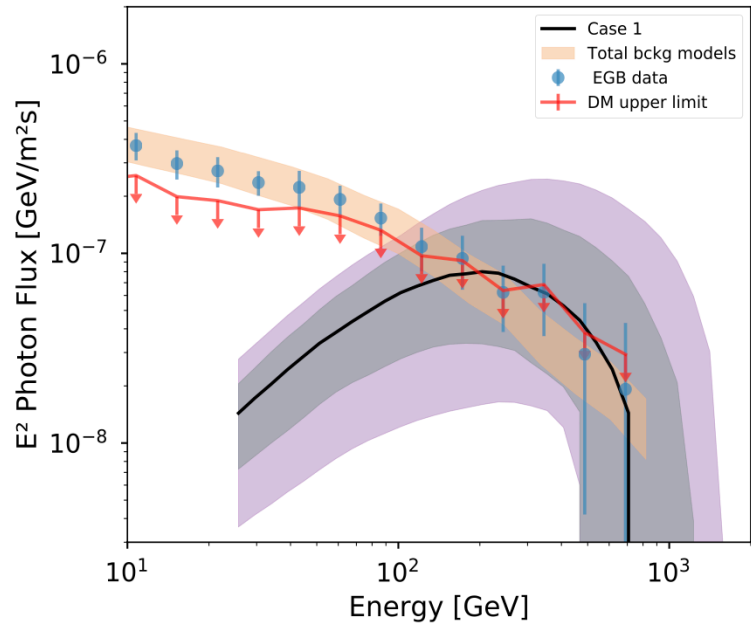
$$M_{ij}^{\nu(1)} \approx \frac{1}{8\pi^2} \lambda_{i23} \lambda_{j32} \frac{m_{\mu} m_{\tau} A_{\tau}}{\tilde{m}^2}$$

$$\approx 2 \times 10^{-2} \text{ eV} \lambda_{i23} \lambda_{j32} \left(\frac{10^8 \text{ GeV}}{\tilde{m}} \right)$$

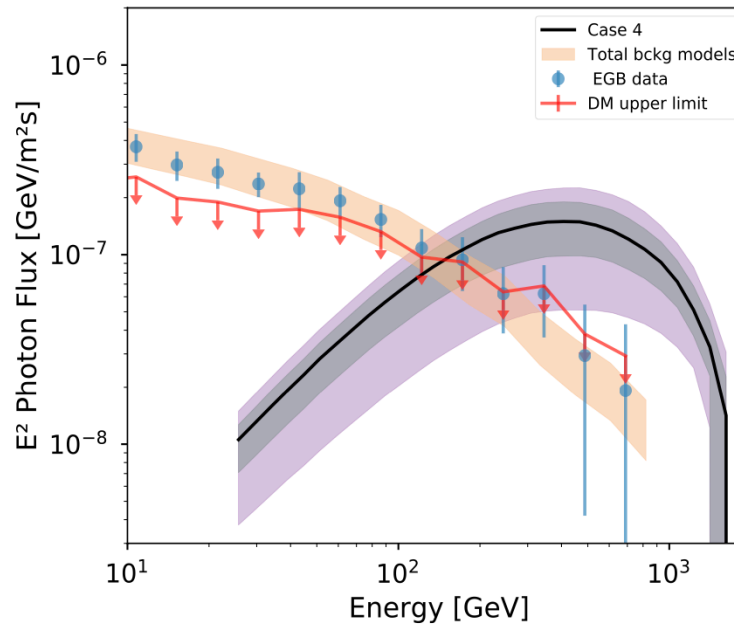
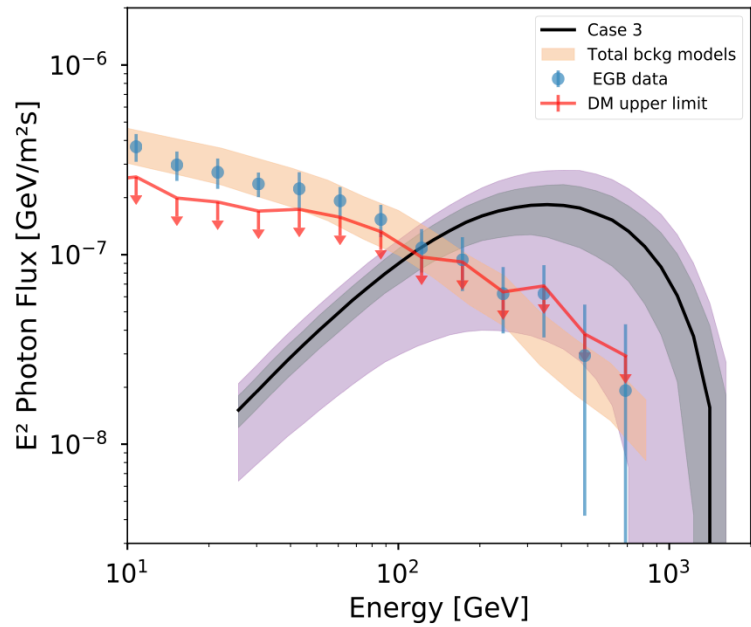
$$\approx 2 \times 10^{-2} \text{ eV} (\lambda_{i23} \lambda_{j32})^{3/4} \left(\frac{4 \times 10^{26} \text{ s}}{\tau_{\tilde{G}}} \right)^{1/4} \left(\frac{2 \text{ TeV}}{m_{\tilde{G}}} \right)^{7/4}$$

Photon Flux

Pure TRpV can explain AMS-02



Another effect:
DAMPE and CALET
can measure all
electron flux to higher
energies.



There is tension be-
tween this explanation
and the photon flux
when we add CALET
and/or DAMPE.

Conclusions

- 1.- In the original Scotogenic model masses of dark matter can be smaller than 500 GeV, as noticed before (in contrast in the IHDM it cannot).
- 2.- In this model, charged and neutral new particles can be long lived.
- 3.- The positron fraction in cosmic rays rises with energy. A decaying Gravitino with mass of a few TeV can explain it. In this case, pure BRpV produce in too many photons.
- 4.- Pure TRpV produce less photons than pure BRpV, and can explain the rise of positron fraction measured by AMS-02. But there is tension between the measurement of different satellites. In addition, neutrino masses and mixing angles should be evaluated.
- 5.- Cosmic rays provide complementary information, thus satellites are an important tool. Particles can reach higher energies, although we loose control.
- 6.- To establish a model beyond the SM we should use a combination of results from different experiments: neutrino, colliders, and satellites.
- 7.- Any possible discrepancy between measurements coming from different satellites might be important and should be resolved.